Oncogene (2008) 27, 5662–5671

www.nature.com/onc

ORIGINAL ARTICLE

Histone H2AX is a critical factor for cellular protection against DNA alkylating agents

JA Meador, M Zhao, Y Su, G Narayan, CR Geard and AS Balajee

Department of Radiation Oncology, College of Physicians and Surgeons, Center for Radiological Research, Columbia University Medical Center, New York, NY, USA

Histone H2A variant H2AX is a dose-dependent suppressor of oncogenic chromosome translocations. H2AX participates in DNA double-strand break repair, but its role in other DNA repair pathways is not known. In this study, role of H2AX in cellular response to alkylation DNA damage was investigated. Cellular sensitivity to two monofunctional alkylating agents (methyl methane sulfonate and *N*-methyl-*N*′-nitro-*N*-nitrosoguanidine (MNNG)) was dependent on H2AX dosage, and H2AX null cells were more sensitive than heterozygous cells. In contrast to wild-type cells, H2AX-deficient cells displayed extensive apoptotic death due to a lack of cell-cycle arrest at G_2/M phase. Lack of G_2/M checkpoint in H2AX null cells correlated well with increased mitotic irregularities involving anaphase bridges and gross chromosomal instability. Observation of elevated poly(ADP) ribose polymerase 1 (PARP-1) cleavage suggests that MNNG-induced apoptosis occurs by PARP-1-dependent manner in H2AX-deficient cells. Consistent with this, increased activities of PARP and poly(ADP) ribose (PAR) polymer synthesis were detected in both H2AX heterozygous and null cells. Further, we demonstrate that the increased PAR synthesis and apoptotic death induced by MNNG in H2AX-deficient cells are due to impaired activation of mitogen-activated protein kinase pathway. Collectively, our novel study demonstrates that H2AX, similar to PARP-1, confers cellular protection against alkylation-induced DNA damage. Therefore, targeting either PARP-1 or histone H2AX may provide an effective way of maximizing the chemotherapeutic value of alkylating agents for cancer treatment.
Oncogene (2008) **27,** 5662–5671; doi:10.1038/onc.2008.187; published online 9 June 2008

Keywords: histone H2AX; poly(ADP) ribose polymerase l; base excision repair; alkylation DNA damage; chromosomal instability; mitogen-activated protein kinase

Correspondence: Dr AS Balajee, Department of Radiation Oncology, College of Physicians and Surgeons, Center for Radiological Research, Columbia University Medical Center, VC-11, Room 239, 168th Street, 630 West, New York, NY 10032, USA.
E-mail: ab836@columbia.edu
Received 2 January 2008; revised 22 April 2008; accepted 4 May 2008; published online 9 June 2008

Introduction

H2AX, a variant form of histone H2A, is rapidly phosphorylated at serine 139 in response to DNA double-strand breaks (DSB) originating from exogenous DNA damage (Rogakou *et al*., 1998, 1999) replication fork collision (Ward and Chen, 2001; Furuta *et al*., 2003), shortened telomeres (Takai *et al*., 2003; d'Adda di Fagagna *et al*., 2003), apoptosis (Rogakou *et al*., 2000) and transcription inhibition (Mischo *et al*., 2005). Phosphorylated histone H2AX, designated as γ-H2AX, forms distinct nuclear foci at or in the vicinity of DSB sites (Rogakou *et al*., 1999). γ-H2AX foci colocalize with many DNA damage-signaling components, including ataxia telangiectasia-mutated (ATM), BRCA1, 53BP1, MDC1, Rad51 and Mre11/Nbs1/Rad50 complex (Fernandez-Capetillo *et al*., 2004). γ-H2AX is important for recruitment and retention of DSB repair factors (Fernandez-Capetillo *et al*., 2002; Celeste *et al*., 2003b) such as Nbs1 (Nijmegen breakage syndrome gene product) and 53BP1 (53 binding protein 1) during the late hours after ionizing radiation (IR). H2AX phosphorylation in response to DSB is mediated by three kinases (Wang *et al*., 2005) belonging to a super family of phosphatidylinositol kinase-like kinases. These include ATM, ATM- and Rad3-related (ATR) and DNA-dependent protein kinase (DNA-PK). Although ATM and DNA-PK are involved in H2AX phosphorylation in an overlapping manner after IR-induced DSB (Stiff *et al*., 2004), H2AX phosphorylation is mainly mediated by ATR after replicative stress (Ward and Chen, 2001).

Two evolutionarily conserved pathways, nonhomologous end joining (NHEJ) and homologous recombination (HR), are involved in the repair of DSB in eukaryotes. Although γ-H2AX is dispensable for DSB recognition (Celeste *et al*., 2003b), available data indicate its importance in the modulation of both NHEJ and HR pathways. Elimination of the serine residue at 129 of H2A at the C-terminal region led to NHEJ impairment in yeast (Downs *et al*., 2000). Also, importance of ser129 of H2A in DNA replication-mediated DSB repair has been demonstrated in *Saccharomyces cerevisiae* (Redon *et al*., 2003). Mice deficient in H2AX are characterized by male-specific infertility, growth retardation and diminished levels of immunoglobulin isotypes (Bassing *et al*., 2002; Celeste

et al., 2002). All these pleiotropic phenotypes have been found associated with enhanced chromosomal instability. Both embryonic stem (ES) and mouse embryonic fibroblasts (MEF) deficient in H2AX showed elevation of spontaneous and IR-induced chromosomal aberrations (Bassing *et al*., 2002; Celeste *et al*., 2002). Spectral karyotypic analysis revealed abnormally high levels of random translocations and complex rearrangements in as many as 24–43% of the metaphases in H2AX null cells as compared to 3–5% in wild-type cells (Celeste *et al*., 2002). Although the fidelity of V(D)J recombination is apparently normal in H2AX-deficient cells, enhanced chromosomal instability indicates that H2AX is required for DNA repair and genomic integrity. Consistent with the genomic instability features, H2AX deficiency has been demonstrated to modify the tumor susceptibility in mice (Bassing *et al*., 2003; Celeste *et al*., 2003a).

H2AX is a critical factor for DNA DSB repair, but its involvement in other DNA repair pathways is not clearly established. In this study, we have evaluated the role of H2AX for the first time in the repair of DNA damage induced by monofunctional alkylating agents. Alkylating agents are mutagenic and genotoxic, and can form adducts with RNA and protein that are likely to contribute to the cytotoxicity (Hurley, 2002). All the major DNA repair mechanisms (base excision repair (BER), nucleotide excision repair, mismatch repair and recombination repair) are involved in the processing of alkylating agent-induced DNA damage (Hoeijmakers, 2001). Any deficiency in these DNA repair pathways can lead to stable mutations leading to cancer, developmental abnormalities and premature aging. Our novel study suggests that H2AX, similar to poly(ADP) ribose polymerase 1 (PARP-1), confers cellular protection against alkylation DNA damage. Further, our study indicates that H2AX is important for cell survival through optimal activation of mitogen-activated protein kinase (MAPK) pathway in response to alkylation DNA damage.

Results

H2AX null cells are extremely sensitive to monofunctional alkylating agents

Data obtained on clonogenic survival after IR treatment in H2AX-proficient and -deficient ES cells were in accordance with a previously published report (Bassing *et al*., 2002). To evaluate the role of H2AX in repair pathways other than DSB, clonogenic survival assay was performed after treatment with alkylating agents (methyl methane sulfonate (MMS) and *N*-methyl-*N*′-nitro-*N*-nitrosoguanidine (MNNG). H2AX-deficient cells showed increased sensitivity to both of these agents. The LC50 value (that reduces the cell survival by 50%) for MMS and MNNG was found to be 0.25 mM and 1.25 μM, respectively for H2AX null cells as compared to 1 mM and 3.1 μM for H2AX-proficient cells. In addition, cell proliferation determined using the CyQuant assay (Figure 1d) revealed a reduction in proliferation by 18.5 and 21.9% after treatment of wild-type cells with 5 and 10 μM of MNNG, respectively. In contrast, proliferation was greatly reduced by MNNG at both concentrations in H2AX null cells (49.7% for 5 μM and 66.4% for 10 μM). H2AX heterozygous cells showed an intermediate response in proliferation after 5 μM (35.1%) and 10 μM (46.4%) of MNNG treatment.

Lack of G_2/M arrest after alkylation DNA damage in H2AX null cells

To verify whether or not the increased sensitivity of H2AX-deficient cells to alkylating agents is due to the lack of G_2/M arrest, cell-cycle analysis was performed in cells of all the three genotypes 48 h after MNNG treatment. Although a modest increase in the proportion of G_2/M cells was observed in both H2AX-proficient and heterozygous cells, H2AX null cells failed to show an efficient G_2/M checkpoint after treatment with a high concentration of MNNG. Consistent with the lack of G_2/M arrest, proportion of sub-G_1 cell population resulting from apoptosis was greatly increased as a function of MNNG dose in H2AX null cells (Figure 2a). This observation was verified by apo-bromodeoxyuridine (BrdU) transferase-mediated dUTP nick end-labeling (TUNEL) assay (Invitrogen, Carlsbad, CA, USA; Figure 2b). Cells labeled by TUNEL assay were analysed by flow cytometry. The frequency of apoptotic cells detected by flow cytometry as sub-G_1 population was highly similar to that detected by Apo-BrdU TUNEL assay. A representative apoptotic cell characterized by typical fragmented chromatin bodies is shown in Figure 2c.

H2AX null cells show mitotic catastrophe after alkylation damage

Observations of the lack of G_2/M checkpoint and increased apoptosis in H2AX null cells after MNNG treatment prompted us to investigate the extent of genomic instability in these cells. For this purpose, anaphase bridges and chromosomal aberrations, which are the characteristic features of mitotic catastrophe, were monitored. Consistent with the lack of G_2/M arrest, increased level of anaphase bridges (48%) was observed 24 h after 5 μM MNNG treatment in H2AX null cells. Further, a large fraction of anaphase and telophase cells showed chromosome fragments that were excluded from the spindle (Figure 3). To determine whether the chromosomal instability is responsible for increased cellular sensitivity, chromosomal aberrations were analysed in H2AX-proficient and -deficient cells. As alkylating agents induce complex exchange-type aberrations, telomere labeling was performed to score the aberrations. Telomere labeling enabled us to identify the orientation of chromosomes in complex exchanges (Figure 4a). The percentages of aberrant metaphases in wild-type cells were found to be 28, 24 and 40%, respectively for 1, 2 and 4 μM of MNNG treatment. In contrast to wild-type cells, 61.5, 68 and 87.5% of the metaphases were found to be aberrant in H2AX null

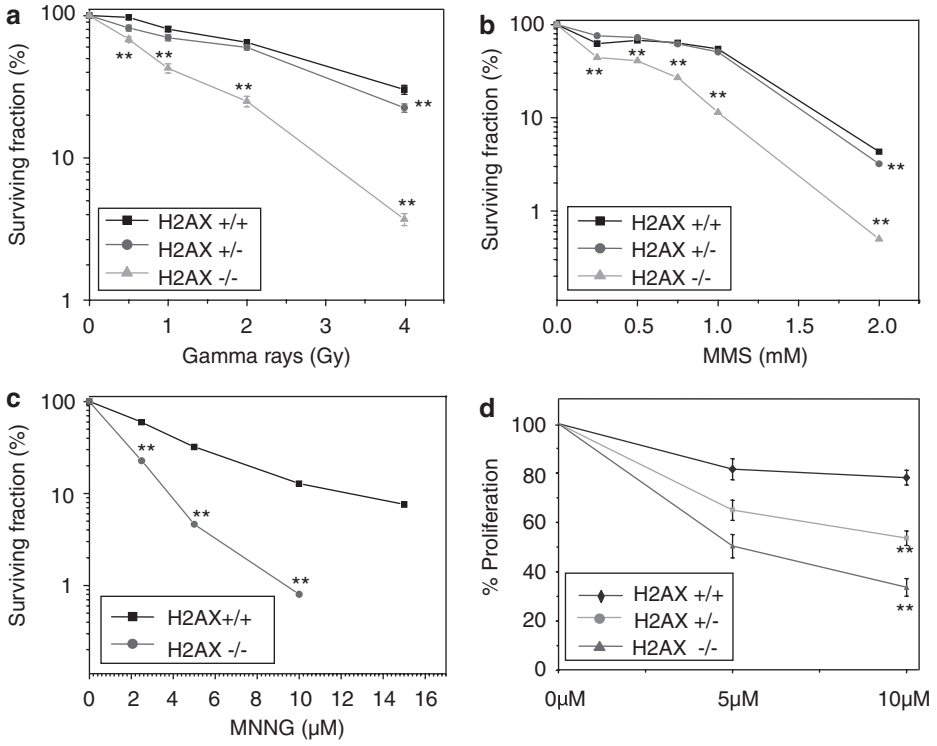

Figure 1 Clonogenic survival assay in H2AX-proficient and -deficient mouse embryonic stem (ES) cells after treatment with γ-rays (**a**), methyl methane sulfonate (MMS) (**b**) and *N*-methyl-*N*′-nitro-*N*-nitrosoguanidine (MNNG) (**c**). ES cells in exponential growth phase were treated with different agents and the cells were allowed to grow for 7–10 days in complete medium for colony formation. CyQuant proliferation assay was performed in H2AX-proficient and -deficient cells 36 h after treatment with the indicated MNNG concentrations (**d**). Data points represent the mean value of at least three independent determinations. Bars indicate the standard error of the mean. H2AX-deficient cells showed more sensitivity than wild-type cells to both alkylating agents. $^{**}P<0.005$.

cells after treatment with 1, 2 and 4 μM MNNG. The frequency of different types of aberrations as well as the total number of aberrations per cell is shown in Figure 4b. The extensive chromosomal instability observed in H2AX null cells after MNNG treatment indicates that H2AX is critical for the maintenance of chromosomal stability after alkylation exposure. In addition, H2AX-deficient cells also showed the lack of 53BP1foci formation after treatment with MNNG (see supplemental data 1; Figure 1).

Alkylation DNA damage triggers PARP-1-mediated apoptosis in H2AX-deficient cells

PARP is an abundant nuclear protein with demonstrated roles in diverse DNA metabolic activities. It is well established that PARP-1 is cleaved in apoptotic cells through the concerted action of caspases 3 and 7 (Soldani and Scovassi, 2002; Bouchard *et al*., 2003) in response to many DNA-damaging agents including MNNG. Therefore, we wished to determine whether the MNNG-induced apoptosis in H2AX-deficient cells occurs via PARP-1 cleavage. Western blot analysis revealed an elevation in the cleaved fragments of PARP-1 (89 and 29 kDa) with increasing concentrations of MNNG in both H2AX heterozygous and null cells analysed 3 h after MNNG treatment (Figure 5a). Similar results were also obtained 24 h after MNNG treatment. In addition to 89 kDa fragment, a ~50 kDa fragment was also detected in all the three cell lines that remained unaltered by MNNG treatment. As PARP-1 is cleaved by caspases 3 and 7, relative levels of full-length and cleaved caspases 3 and 7 were subsequently examined in cells of all the three genotypes treated with 10 and 20 μM MNNG (Figure 5b). Consistent with elevated PARP-1 cleavage, increased level of cleaved caspases was observed in both H2AX heterozygous and null cells 24 h after MNNG treatment. These results clearly demonstrate that MNNG-induced apoptosis occurs by PARP-1-mediated pathway in H2AX-deficient cells. In contrast to caspases 3 and 7, caspase 9, which is dispensable for PARP-1-mediated apoptosis, remained essentially unaltered in both sham- and MNNG-treated cells of all the three genotypes (Figure 5b).

H2AX-deficient cells show increased PARP-1 activity and PAR synthesis

In response to DNA damage, PARP-1 is activated and catalyses the synthesis of poly(ADP) ribose (PAR) polymers that are covalently attached to a number of acceptor proteins. The main protein among them is PARP-1 itself. To determine whether PARP activity is altered in H2AX-deficient cells after MMNG damage, PARP activity was determined in the whole-cell extracts prepared from sham- and MNNG-treated cells. PARP activity assay was performed essentially according to the manufacturer's protocol (R&D Systems, Minneapolis,

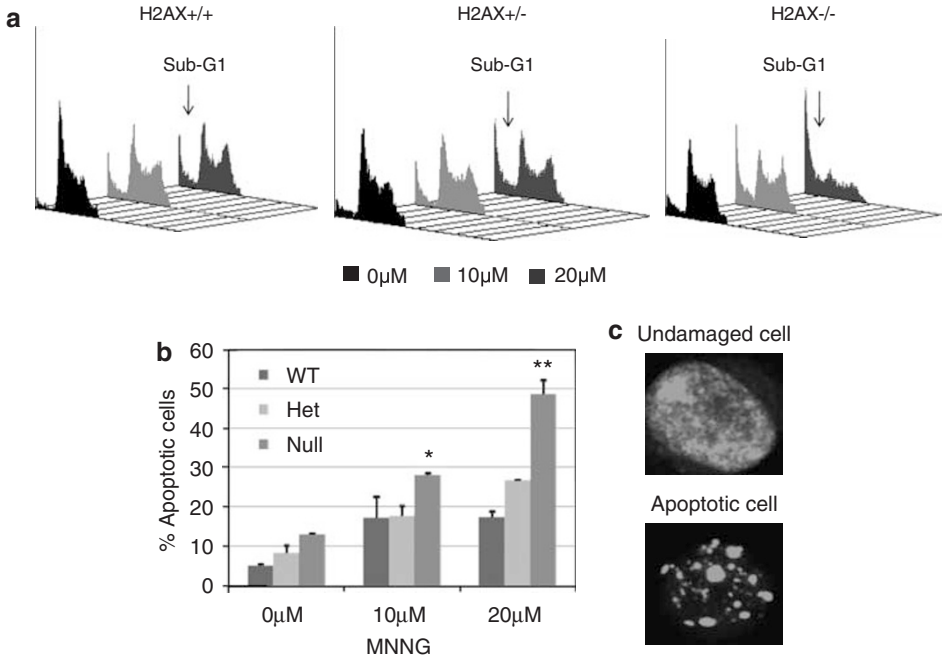

Figure 2 Analysis of cell-cycle progression in H2AX-proficient and -deficient cells after exposure to *N*-methyl-*N*′-nitro-*N*-nitrosoguanidine (MNNG). Cells in exponential growth phase were treated with MNNG (10 and 20 μM) for 90 min and post-incubated in drug-free medium for 48 h (**a**). The cells were fixed and analysed by flow cytometry. The percentage of apoptotic cells detected as sub-G_1 population by flow cytometry correlated well with the fraction of apoptotic cells detected by apo-bromodeoxyuridine (BrdU) transferase-mediated dUTP nick end-labeling (TUNEL) assay. Therefore, the data are pooled and presented in the form of histogram (**b**). MNNG-induced apoptosis was found to be dependent on H2AX dosage. A representative apoptotic cell with characteristic pattern of DNA fragmentation induced by 10 μM MNNG in H2AX null cell line is shown in the bottom right panel (**c**). $*P<0.05$; $**P<0.005$.

MN, USA). Even in the absence of exogenous damage, PARP activity was higher both in H2AX heterozygous and null cells in comparison to H2AX-proficient cells. Although, PARP activity measured after 3 and 24 h of MNNG treatment showed a gradual decline in all the three genotypes, PARP activity in H2AX-deficient cells was higher than that of H2AX-proficient cells (Figure 6a). As PARP-1 is responsible for bulk of PARP activity, we wished to determine whether the increased PARP activity observed in unchallenged H2AX heterozygous and null cells is due to increased PARP-1 expression. For this purpose, PARP-1 expression was monitored both at the mRNA and protein levels. Consistent with increased PARP activity, PARP-1 expression detected by reverse transcription (RT)–PCR and western blot analyses was higher in both heterozygous and homozygous cells deficient in H2AX (Figure 6b). These data clearly demonstrate a close correlation between increased PARP activity and increased PARP-1 expression in H2AX-deficient cells. It is unclear at this point whether elevated PARP-1 level is due to increased stability of PARP-1 mRNA and protein in H2AX-deficient cells. We next examined whether or not PAR synthesis is also increased in H2AX-deficient cells with and without MNNG treatment. Western blot analysis was performed using a PAR antibody (mouse monoclonal immunoglobulin G; Trevigen, Gaithersburg, MD, USA). In corroboration with increased PARP activity, increased levels of PAR synthesis were detected in both H2AX heterozygous- and homozygous-deficient cells either with or without MNNG treatment (see supplemental data 1, Figure 2).

MNNG impairs the activation of MAPK signaling pathway in H2AX-deficient cells

A recent study has shown that the massive PAR synthesis induced by MNNG treatment leads to apoptotic death through downregulation of phosphorylated extracellular signal-related kinase (ERK1 and ERK2) proteins, which are members of MAPK signal transduction pathway (Ethier *et al*., 2007). In the light of this observation, it is important to determine whether or not similar effect of PAR synthesis on MAPK pathway is observed in H2AX-deficient cells. To address this issue, western blot analysis was performed using the total cellular proteins isolated from sham- and MNNG-treated H2AX-proficient and -deficient cells at 3 and 24 h postrecovery times. H2AX-proficient cells did not show any alteration in the relative levels of ERK1 and ERK2 phosphorylation either with or without MNNG treatment, In contrast, phosphorylation levels of both ERK1 and ERK2 proteins were greatly reduced with increasing MNNG concentrations in both heterozygous and null cells at both recovery times (Figure 7). However, the total cellular levels of unmodified ERK1 and ERK2 proteins did not show much alteration in all the three cell lines. This observation illustrates that H2AX is critical for the optimal activation and persistence of MAPK pathway after alkylation DNA damage. Interestingly, a clear H2AX dose-dependent effect was also observed in the phosphorylated ERK1 and ERK2 proteins even in undamaged cells. Collectively, our novel study highlights the importance of H2AX in the regulation of MAPK signal transduction

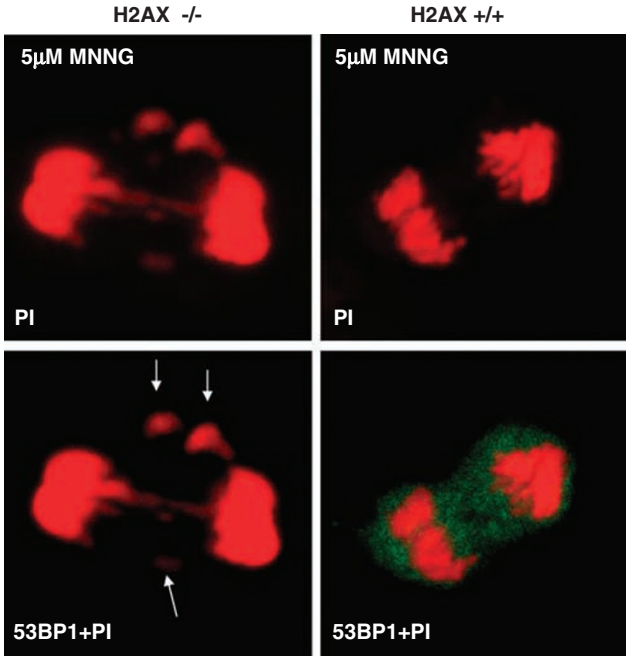

Figure 3 H2AX-deficient cells show mitotic irregularities after *N*-methyl-*N*′-nitro-*N*-nitrosoguanidine (MNNG) treatment. H2AX-proficient and -deficient cells grown on chamber slides were treated with 5 μM MNNG for 90 min and post-incubated in drug-free medium for 24 and 48 h. Cells were fixed in acetone:methanol (1:1) and immunostained for 53BP1 using a primary rabbit antibody (Novus Biologicals) and a fluorescein conjugated secondary antibody (Vector Laboratories). Nuclei were counterstained with propidium iodide (PI). Note the anaphase bridge and chromosome fragments (arrows) in MNNG-treated H2AX null cells.

pathway. Elucidation of the precise molecular link between MAPK and H2AX awaits further investigations.

Discussion

H2AX is rapidly phosphorylated at serine 139 in response to DSB generated by IR (Rogakou *et al*., 1998, 1999) and stalled replication forks (Ward and Chen, 2001; Furuta *et al*., 2003). H2AX is an essential DSB repair factor, but its role in other DNA repair pathways is largely unknown. This study provides the novel evidence for the critical importance of H2AX in cellular protection against alkylation DNA damage.

DNA alkylating agents are widely used in cancer therapy and mismatch repair-deficient cancer cells show resistance to cisplatin and alkylating agents such as MNNG (Aebi *et al*., 1997; Karran *et al*., 2003). Therefore, identification of key genetic factors responsible for cellular defense against alkylation damage is critical for improving the efficiency of cancer treatment. A previous study has shown that 95 and 79% of total DNA methylation is generated by MMS and MNNG, respectively (Beranek, 1990) and these modified bases (*N*7-methylguanine, *N*3-methyladenine and *N*3-methylguanine) are removed by BER pathway (Mitra and Kaina, 1993). Analogous to H2AX-deficient cells, DNA polymerase β (an important BER factor)-deficient cells show increased apoptosis and chromosome breakage upon exposure to alkylating agents (Ochs *et al*., 1999; Horton *et al*., 2005). Similarities observed in terms of alkylation DNA damage-induced cell killing and chromosomal aberrations between DNA polymerase β and H2AX-deficient cells strongly suggest that H2AX cells may be deficient in BER activity.

Our study has unraveled an interesting molecular link between H2AX and PARP-1 in response to alkylation DNA damage. In contrast to wild-type cells, H2AX-deficient cells show increased PARP activity and PAR synthesis even in the absence of exogenous DNA damage. Further, apoptosis induced by MNNG occurs in a PARP-1-mediated manner in H2AX-deficient cells. Elevated PARP activity and PAR synthesis observed in H2AX-deficient cells suggest a role for H2AX in the regulation of PARP activity. The deregulation of PARP activity may be responsible for the abnormal cellular response of H2AX-deficient cells to MMS and MNNG. In the present study, increased level of ribosylated PARP-1 detected both in H2AX heterozygous and null cells for an extended period of time (24 h after treatment) indicates that H2AX is important for maintaining the balance between PARP and PARG system after alkylation DNA damage. The extreme sensitivity of both PARP-1- and H2AX-deficient cells to MMS and MMNG strongly indicate the critical requirement of both of these gene products for cellular defense against alkylating agents.

Requirement for H2AX in G_2/M arrest after low doses of low LET radiation (0.5–2.5 Gy) was demonstrated earlier (Fernandez-Capetillo *et al*., 2002). Similarly, requirement of ATM kinase for low-dose radiation-induced G_2/M checkpoint was also reported (Xu *et al*., 2002). In this study, lack of G_2/M arrest was demonstrated in H2AX-deficient cells after treatment with a high dose of MNNG (20 μM). A recent paper has shown that MNNG activates cell-cycle checkpoints in a dose-dependent manner (Beardsley *et al*., 2005) and Chk2 was found to be dispensable for the checkpoint induced by 25 μM MNNG. Although both IR and MNNG induce DSB, their mode of induction is distinctly different. IR directly induces DSB, whereas DSB generated by MNNG are due to simultaneous processing of clustered AP (apurinic/apyrimidinic) sites on opposite DNA strands (Lomax *et al*., 2004). Further, MNNG induces DSB only in S-phase cells and the DSB abundance after MNNG treatment may depend on the initial lesion load. Due to differences in the mode of DSB induction by IR and MNNG, it is logical to assume that the yield of DSB may considerably differ between the two treatment conditions. Beardsley *et al*. (2005) demonstrated the requirement of ATR and Chk1 for G_2/M arrest imposed by high dose of MNNG. It would be interesting to determine whether the loss of G_2/M arrest after MNNG treatment (20 μM) is due to impaired activation of ATR and Chk1 in H2AX-deficient cells. Increased frequencies of anaphase bridges and chromosome fragments resulting from the alkylation

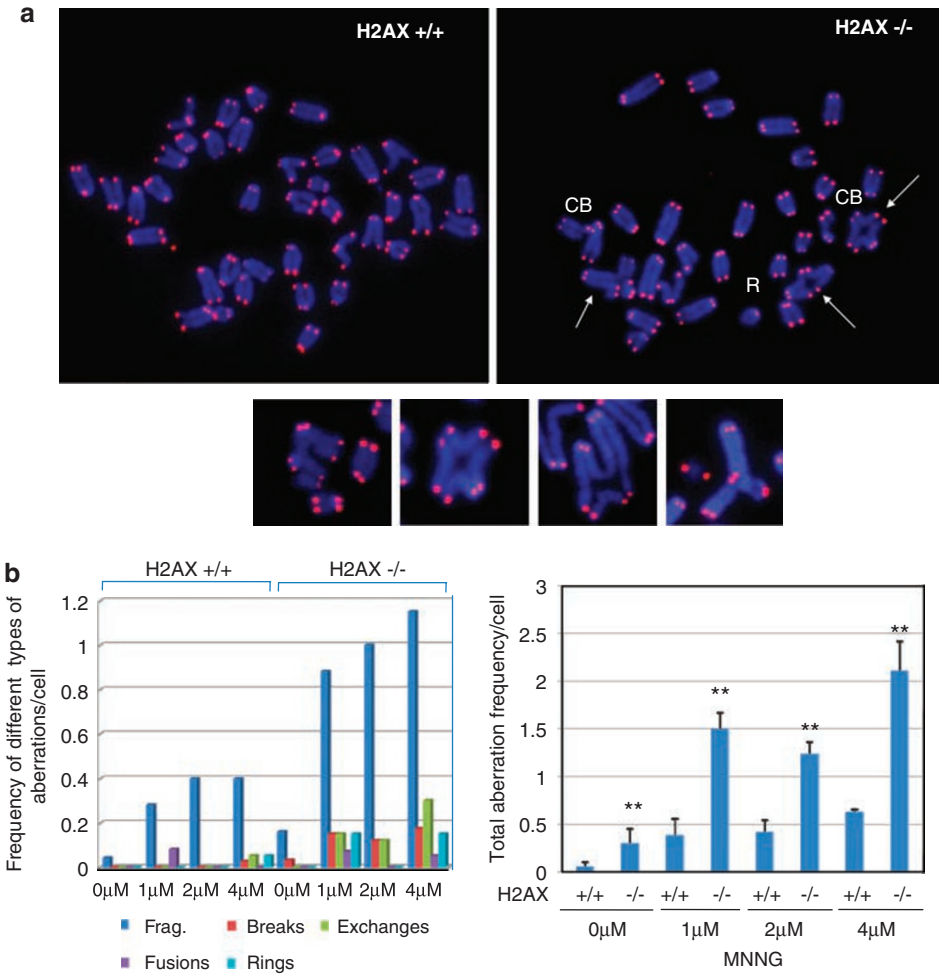

Figure 4 H2AX null cells show increased chromosomal instability after alkylating agent exposure (**a**). Cells in exponential growth phase were treated with different concentrations of *N*-methyl-*N*′-nitro-*N*-nitrosoguanidine (MNNG) (1, 2 and 4 μM) for 3 h. Metaphase chromosomes were prepared 24 h following treatment. Metaphase chromosomes were labeled with Cy3-labeled telomere-specific PNA probe and the chromosomal aberrations were analysed using an epifluorescence microscope (Nikon). Arrows indicate the complex exchange-type aberrations. The complex exchange-type aberrations observed in H2AX null cells is shown in the bottom panel. CB, chromatid break; R, ring. The frequency of different types of chromosome aberrations observed per cell and the frequency of total aberrations observed per cell are shown in the form of histograms (**b**). The total yield of aberrations observed per metaphase in H2AX null cells was compared to wild-type cells. $^{**}P<0.005$.

DNA damage in H2AX-deficient cells are suggestive of premature progression of damaged cells from G_2 to mitosis. These results also highlight the importance of H2AX in the maintenance of proper chromosome segregation and stability. Our finding together with the recent demonstration of γ-H2AX enriched in mitotic cells (Ichijima *et al*., 2005; McManus and Hendzel, 2005) indicate that H2AX is important for mitotic cell integrity. Collectively, this study reveals that in addition to being a regulatory factor for PARP-1 activation, H2AX also participates in maintaining the chromosomal stability through regulation of G_2/M checkpoint control.

MAPK family members, that include ERK1 and ERK2, c-Jun N-terminal kinase and p38, have been shown to be activated by different types of external stimuli (Tibbles and Woodgett, 1999). Requirement for ERK1 and ERK2 activation has been demonstrated for DNA damage-induced G_2/M arrest in mammalian cells (Chou *et al*., 2007; Yan *et al*., 2007). In this study, we demonstrated that the lack of activation and persistence of phosphorylated ERK1 and ERK2 proteins after alkylation damage correlate with lack of G_2/M arrest in H2AX-deficient cells. A recent study has demonstrated the correlation between PAR synthesis and ERK1/ERK2 activation after treatment with a high concentration of MNNG (100 μM) in HeLa cells (Ethier *et al*., 2007). Inhibition of PAR synthesis by PARP-1 inhibitor prevents the loss of phosphorylation of ERK1/ERK2 and confers cellular protection against MNNG treatment. Also, inhibition of ERK1/ERK2 phosphorylation by UO126 resulted in the elevation of MNNG-induced apoptotic death in HeLa cells. A few recent studies have unraveled the molecular interplay between PARP-1 and ERK1/ERK2 and the activation of PARP-1 and ERK1/ERK2 seems to be interdependent (Kauppinen *et al*., 2006; Cohen-Armon *et al*., 2007). In the present study, we observed the lack of activation and persistence of ERK1/ERK2 phosphorylation even at low concentrations

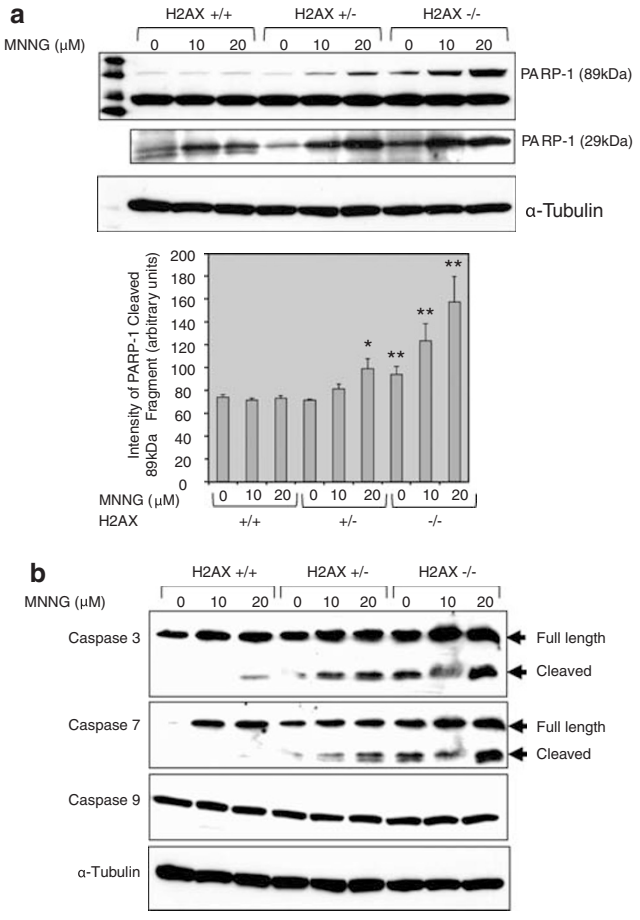

Figure 5 *N*-methyl-*N*′-nitro-*N*-nitrosoguanidine (MNNG)-induced apoptosis occurs in a PARP-1-dependent manner in H2AX-deficient cells. Cells in exponential growth were treated with MNNG at the indicated concentrations and the total cellular proteins were extracted from cells at 3 and 24 h after treatment. Western blot analysis was performed using 40 μg of proteins and PARP-1 cleavage was detected using an antibody specific for 89 kDa (Cell signaling technology) and 29 kDa (Abcam) fragments of PARP-1. The intensities of 89 and 29 kDa fragments increased in H2AX-deficient cells in a H2AX dose-dependent manner after MNNG treatment (**a**). Densitometric measurement of 89 kDa PARP-1 fragment observed in H2AX-proficient and -deficient cells with and without MNNG treatment is shown in the bottom panel. Cleaved fragment of PARP-1 (89 kDa) was more pronounced in heterozygous and homozygous H2AX-deficient cells than wild-type cells. (**b**) Western blot analysis of full-length and cleaved caspases 3, 7 and 9 in sham- and MNNG-treated H2AX-proficient and -deficient cells is shown. α-Tubulin was used to verify the loading of equal amounts of proteins for all the three genotypes. $*P<0.05$; $**P<0.005$.

of MNNG in H2AX-deficient cells. Interestingly, phosphorylation level of ERK1/ERK2 proteins was also found reduced in H2AX heterozygous and null cells in the absence of MNNG treatment. This observation clearly points out that H2AX is required for the optimal activation of MAPK pathway. Future studies are required to understand the mechanism for the regulation of MAPK pathway by H2AX.

Observation of H2AX dose-dependent cytotoxic effects of alkylating agents in heterozygous and homozygous cells indicates that PARP-1 activity is deregulated by the absence of H2AX. This study provides evidence that H2AX is a critical factor for cellular protection against alkylating agents through regulation of PARP-1 activity. The intrinsic molecular interplay between PARP-1 and H2AX may be important for the coordinated regulation of signal transduction, cell-cycle and DNA repair activities in response to alkylation DNA damage. Owing to their importance in cellular protection against alkylation damage, targeting either PARP-1 or histone H2AX may provide an effective way of maximizing the chemotherapeutic value of alkylating agents for cancer treatment.

Materials and methods

Cell lines and culture conditions

Mouse ES cells differing in the functional status of H2AX (wild type (+/+), heterozygous (+/−) and null (−/−)) were generously provided by Dr CH Bassing and Dr FW Alt (Department of Genetics, The CBR Institute for Biomedical Research, The Children's Hospital, Harvard Medical School, Boston, MA, USA). Procedures followed for the generation and propagation of these cells lines have been described by Bassing *et al*. (2002). Cells were routinely cultured in knockout DMEM (Invitrogen) supplemented with 10% ES-tested fetal bovine serum. Other components of the medium for ES cell culture were essentially the same as described by Bassing *et al*. (2002).

Treatment of ES cells, clonogenic survival assay and immunofluorescence analysis

To determine the sensitivity of H2AX-proficient and -deficient (heterozygous and homozygous) cells to alkylating agents, clonogenic survival experiments were performed. For survival experiment, 1×10^3 cells from wild-type H2AX, heterozygous and null cell lines were seeded in 0.1% gelatin-coated 6 cm dishes 18 h prior to treatment. For alkylation damage, cells were treated with indicated concentrations of MMS and MNNG for 3 h. Cells were washed once in complete medium and incubated in drug-free medium for 7–10 days and colonies were fixed in 70% ethanol and stained with Coomassie brilliant blue (0.5%). For comparison, survival experiment with different doses of γ-rays (0.5, 1, 2 and 4 Gy) was performed (Gamma Cell 40; Atomic Energy of Canada, Chalkriver, Ontario, Canada). At least three independent determinations were made for each treatment condition. Immunofluorescence staining of 53BP1 (Novus Biologicals, Littleton, CO, USA) was performed essentially as described before (Balajee and Geard, 2001, 2004).

Cell-cycle analysis

For cell-cycle analysis, H2AX wild-type, heterozygous and null cells were seeded at a density of 500 000 cells in 10 cm culture dishes 18 h prior to treatment. Cells were treated with MNNG for 90 min at 37 °C. Cells after different post-incubation times (24 and 48 h) were trypsinized, washed once in phosphate-buffered saline (PBS) and fixed in 70% ethanol. Samples were analysed using a Becton Dickinson (Franklin Lakes, NJ, USA) FACSCalibur and at least 10 000 events were recorded for each sample.

Effect of MNNG on Cell proliferation by CyQuant assay

Cells from all the three genetic backgrounds were seeded into 96-wells plate at a density of 7500 cells per well in 200 μl of

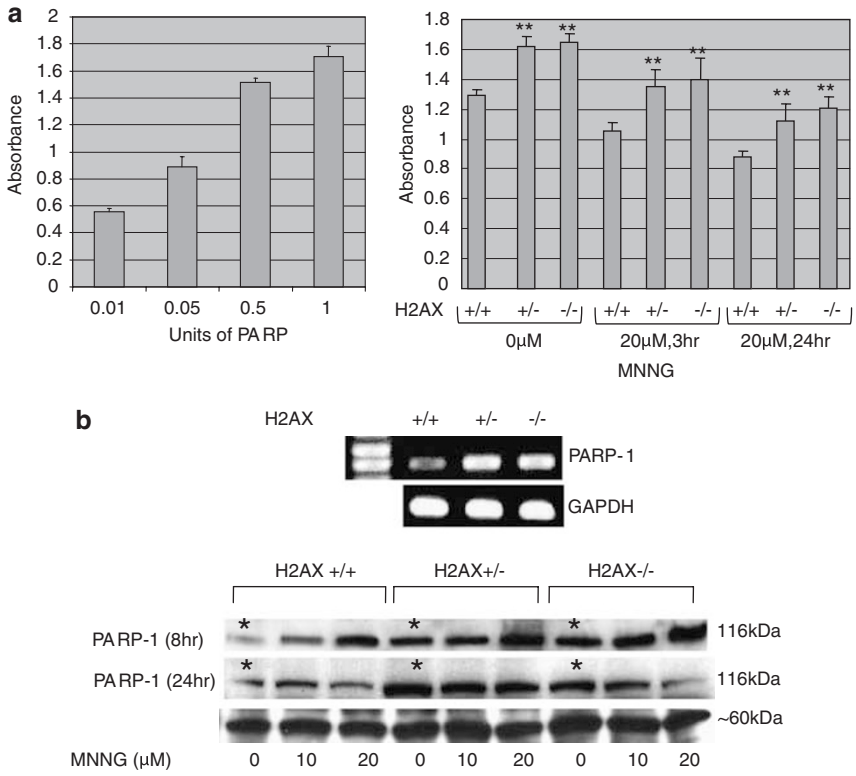

Figure 6 PARP activity is elevated in H2AX-deficient cells. Cells in exponential growth were either sham-treated or treated with *N*-methyl-*N*′-nitro-*N*-nitrosoguanidine (MNNG) (10 and 20 μM) for 90 min and post-incubated in drug-free medium for the indicated times. Total cellular proteins were isolated at 3 and 24 h after treatment and the PARP activity was determined using a colorimetric assay essentially following the manufacturer's instructions. Biotinylated histone substrate was used to measure PARP activity. PARP activity was determined by measuring the absorbance at 450 nm with a microplate reader (Biotek Synergy 2). The standard curve obtained using purified PARP is shown in the left panel and the PARP activity measured in cells is displayed in the right panel (**a**). Bars indicate the standard error of the mean of at least three determinations for each treatment condition $^{**}P<0.005$. (**b**) PARP-1 expression was determined in H2AX-proficient and -deficient cells at the mRNA and protein levels by reverse transcription (RT)–PCR and western blot analyses. RT–PCR analysis was performed using a standard procedure. PARP-1 expression in sham– and MNNG-treated cells was monitored by western blot using 40 μg of total cellular proteins. Total cellular proteins were isolated 8 and 24 h after MNNG treatment. A nonspecific band detected at ~60 kDa was used to verify the equal loading of proteins. PARP-1 expression level observed in all the three cell lines is indicated by asterisks.

DMEM knockout media and incubated at 37 °C for 18 h. Cells were treated with increasing concentrations of MNNG (5 or 10 μM) for 90 min. Effect of MNNG on cell proliferation was assayed 36 h later by CyQuant assay (Invitrogen) following the manufacturer's instructions.

Detection of apoptosis by Apo-BrdU TUNEL assay
For the determination of apoptotic cells, an apo-BrdU TUNEL assay (Invitrogen) was performed. Cells were trypsinized and DNA break sites were labeled by Apo-BrdU kit following the manufacturer's protocol (Molecular Probes, Carlsbad, CA, USA). Cells labeled with fluorescein were analysed by FACSCalibur and FACScan software (Becton Dickinson, Franklin Lakes, NJ, USA).

Analysis of chromosomal aberrations and anaphase bridges
Cells in exponential growth phase were treated with different concentrations of MNNG (1–5 μM) and post-incubated for 24 h. Cells were arrested at mitosis by the addition of Karyomax colcemid (0.05 μg/ml; Gibco, Carlsbad, CA, USA) for the last 3 h and the metaphase chromosomes were prepared using the standard procedure. Chromosomes were hybridized with telomeric DNA-specific Cy3-labeled peptide nucleic acid probe and the aberrations were scored. For the estimation of anaphase bridges, cells were seeded in two-well chamber slides, treated with MNNG and post-incubated for 24 h. Cells were fixed in acetone:methanol (1:1) and immunostained for 53BP1. Slides were stained with propidium iodide (0.5 μg/ml) and the anaphase bridges were scored in mitotic cells.

Western blot analysis
Primary antibodies were obtained from commercial sources (PARP-1 and cleaved PARP from Cell Signaling Technology (Danvers, MA, USA) and Abcam (Cambridge, MA, USA); PAR from Trevigen; phosphorylated and nonphosphorylated ERK1 and ERK2 from Cell Signaling Technology and actin, α-tubulin and glyceraldehyde-3-phosphate dehydrogenase (GAPDH) from Santa Cruz Biotechnology (Santa Cruz, CA, USA)). Horseradish peroxidase-conjugated secondary antibodies for anti-mouse and anti-rabbit were procured from Vector Laboratories (Burlingame, CA, USA). Equal amount of proteins (40 μg) isolated from H2AX-proficient and -deficient cells were loaded onto either linear (8%) or gradient (4–12% and 4–20%) polyacrylamide–SDS gels and the proteins were transferred onto polyvinylidene fluoride membranes (Invitrogen). The signal was detected using enhanced

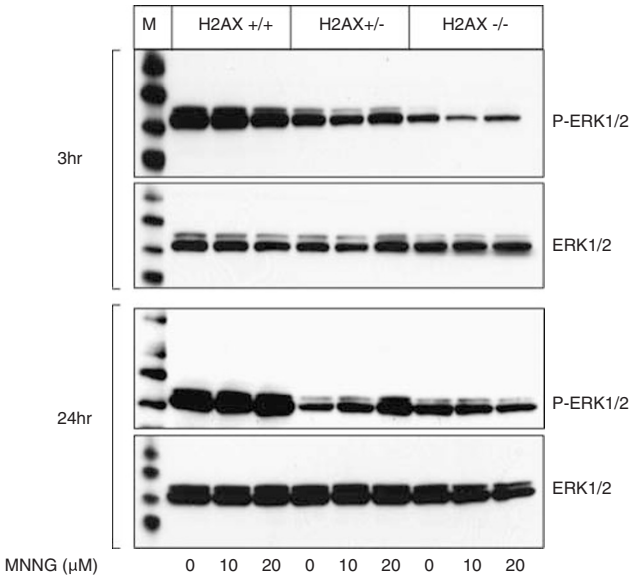

Figure 7 H2AX is required for the optimal activation of MAPK pathway after alkylation DNA damage. Cells in exponential growth phase were either sham- or *N*-methyl-*N*′-nitro-*N*-nitrosoguanidine (MNNG)-treated and the proteins were isolated at 3 and 24 h after treatment. Western blot analysis was performed using antibodies specific for phosphorylated and nonphosphorylated forms of ERK1 and ERK2. Note the impairment in the activation and persistence of phosphorylated forms of ERK1 and ERK2 in H2AX-deficient cells with increasing MNNG concentrations.

chemiluminescence (ECL Plus; Amersham, Piscataway, NJ, USA) method following the manufacturer's instructions.

Quantification of PARP activity in whole-cell extracts
PARP activity kit (R&D Systems) was used to measure the incorporation of biotinylated PAR into histone proteins. Cellular proteins prepared from sham- and MNNG-treated cells were used for the measurement of PARP activity. First 25 μl of 1 × PARP cocktail was added to each well. After adding 20 μg protein and corresponding volume of PARP-HSA enzyme to final volume of 50 μl, the plate was incubated at room temperature for 60 min, then washed four times with 1 × PBS (200 μl per well) and 50 μl of Strep-HRP per well was added. The plate was incubated for 20 min at room temperature and washed four times with 1 × PBS followed by the addition of 50 μl of TACS-Sapphire to each well. The plate was incubated for 20–30 min in dark and the absorbance was read at 450 nM with a microplate reader. The experiment was performed in triplicates for each treatment condition and postrecovery time.

Analysis of PARP-1 expression by RT–PCR
Total cellular RNA was isolated using TRIzol reagent (Invitrogen). Total cellular RNA (1–2 μg) was used for cDNA synthesis following the manufacturer's instructions (Cloned AMV first-strand synthesis kit; Invitrogen). RT–PCR was carried out for PARP-1 detection using the forward and reverse primers (5′-GCAGCGAGAGTATTCCCAAG-3′; 5′-CCGTCTTCTTGACCTTCTGC-3′). Commercially available primers were used to monitor the expression of GAPDH (Super Array, Frederick, MD, USA).

Statistical analysis
Experimental data were generated from at least three independent determinations for most of the biological end points studied. Statistical significance was estimated by subjecting the data to two-tailed Student's *t*-test using Microsoft Excel software. For all analyses, data sets obtained for H2AX heterozygous- and homozygous-deficient cells were compared with H2AX-proficient wild-type cells. Statistical significance was accepted at $P<0.05$. *P*-value is indicated in the form of asterisks in the figures ($*P<0.05$; $**P<0.005$).

Acknowledgements

We acknowledge the generous gift of mouse ES cells proficient and deficient in H2AX from Dr CH Bassing and Dr FW Alt at the Department of Genetics, The CBR Institute for Biomedical Research, The Children's Hospital, Harvard Medical School, Boston, MA, USA. This study was partially supported by a research grant from US Department of Energy, Office of Sciences (BER) awarded to ASB (DE-FG02-05ER64055) and CRG (DE-FG 02-05ER 64054). ASB and CRG acknowledge the financial support received from NIH/NCI (5P01CA49062-16).

References

Aebi S, Fink D, Gordon R, Kim HK, Zheng H, Fink JL *et al*. (1997). Resistance to cytotoxic drugs in DNA mismatch repair-deficient cells. *Clin Cancer Res* **3**: 1763–1767.

Balajee AS, Geard CR. (2001). Chromatin-bound PCNA complex formation triggered by DNA damage occurs independent of the ATM gene product in human cells. *Nucleic Acids Res* **29**: 1341–1351.

Balajee AS, Geard CR. (2004). Replication protein A and gamma-H2AX foci assembly is triggered by cellular response to DNA double-strand breaks. *Exp Cell Res* **300**: 320–334.

Bassing CH, Chua KF, Sekiguchi J, Suh H, Whitlow SR, Fleming JC *et al*. (2002). Increased ionizing radiation sensitivity and genomic instability in the absence of histone H2AX. *Proc Natl Acad Sci USA* **99**: 8173–8178.

Bassing CH, Suh H, Ferguson DO, Chua KF, Manis J, Eckersdorff M *et al*. (2003). Histone H2AX: a dosage-dependent suppressor of oncogenic translocations and tumors. *Cell* **114**: 359–370.

Beardsley DI, Kim WJ, Brown KD. (2005). *N*-methyl-*N*′-nitro-*N*-nitrosoguanidine activates cell-cycle arrest through distinct mechanisms activated in a dose-dependent manner. *Mol Pharmacol* **68**: 1049–1060.

Beranek DT. (1990). Distribution of methyl and ethyl adducts following alkylation with monofunctional alkylating agents. *Mutat Res* **231**: 11–30.

Bouchard VJ, Rouleau M, Poirier GG. (2003). PARP-1, a determinant of cell survival in response to DNA damage. *Exp Hematol* **31**: 446–454.

Celeste A, Difilippantonio S, Difilippantonio MJ, Fernandez-Capetillo O, Pilch DR, Sedelnikova OA *et al*. (2003a). H2AX haploinsufficiency modifies genomic stability and tumor susceptibility. *Cell* **114**: 371–383.

Celeste A, Fernandez-Capetillo O, Kruhlak MJ, Pilch DR, Staudt DW, Lee A *et al*. (2003b). Histone H2AX phosphorylation is dispensable for the initial recognition of DNA breaks. *Nat Cell Biol* **5**: 675–679.

Celeste A, Petersen S, Romanienko PJ, Fernandez-Capetillo O, Chen HT, Sedelnikova OA *et al*. (2002). Genomic instability in mice lacking histone H2AX. *Science* **296**: 922–927.

Chou YH, Ho YS, Wu CC, Chai CY, Chen SC, Lee CH *et al*. (2007). Tubulozole-induced G_2/M cell cycle arrest in human colon cancer cells

through formation of microtubule polymerization mediated by ERK1/2 and Chk1 kinase activation. *Food Chem Toxicol* **45**: 1356–1367.

Cohen-Armon M, Visochek L, Rozensal D, Kalal A, Geistrikh I, Klein R *et al*. (2007). DNA-independent PARP-1 activation by phosphorylated ERK2 increases Elk1 activity: a link to histone acetylation. *Mol Cell* **25**: 297–308.

d'Adda di Fagagna F, Reaper PM, Clay-Farrace L, Fiegler H, Carr P, Von Zglinicki T *et al*. (2003). A DNA damage checkpoint response in telomere-initiated senescence. *Nature* **426**: 194–198.

Downs JA, Lowndes NF, Jackson SP. (2000). A role for *Saccharomyces cerevisiae* histone H2A in DNA repair. *Nature* **408**: 1001–1004.

Ethier C, Labelle Y, Poirier GG. (2007). PARP-1-induced cell death through inhibition of the MEK/ERK pathway in MNNG-treated HeLa cells. *Apoptosis* **12**: 2037–2049.

Fernandez-Capetillo O, Chen HT, Celeste A, Ward I, Romanienko PJ, Morales JC *et al*. (2002). DNA damage-induced G_2-M checkpoint activation by histone H2AX and 53BP1. *Nat Cell Biol* **4**: 993–997.

Fernandez-Capetillo O, Lee A, Nussenzweig M, Nussenzweig A. (2004). H2AX: the histone guardian of the genome. *DNA Repair (Amst)* **3**: 959–967.

Furuta T, Takemura H, Liao ZY, Aune GJ, Redon C, Sedelnikova OA *et al*. (2003). Phosphorylation of histone H2AX and activation of Mre11, Rad50, and Nbs1 in response to replication-dependent DNA double-strand breaks induced by mammalian DNA topoisomerase I cleavage complexes. *J Biol Chem* **278**: 20303–20312.

Hoeijmakers JH. (2001). Genome maintenance mechanisms for preventing cancer. *Nature* **411**: 366–374.

Horton JK, Stefanick DF, Naron JM, Kedar PS, Wilson SH. (2005). Poly(ADP-ribose) polymerase activity prevents signaling pathways for cell cycle arrest after DNA methylating agent exposure. *J Biol Chem* **280**: 15773–15785.

Hurley LH. (2002). DNA and its associated processes as targets for cancer therapy. *Nat Rev Cancer* **2**: 188–200.

Ichijima Y, Sakasai R, Okita N, Asahina K, Mizutani S, Teraoka H. (2005). Phosphorylation of histone H2AX at M phase in human cells without DNA damage response. *Biochem Biophys Res Commun* **336**: 807–812.

Karran P, Offman J, Bignami M. (2003). Human mismatch repair, drug-induced DNA damage, and secondary cancer. *Biochimie* **85**: 1149–1160.

Kauppinen TM, Chan WY, Suh SW, Wiggins AK, Huang EJ, Swanson RA. (2006). Direct phosphorylation and regulation of poly(ADP-ribose) polymerase-1 by extracellular signal-regulated kinases 1/2. *Proc Natl Acad Sci USA* **103**: 7136–7141.

Lomax ME, Cunniffe S, O'Neill P. (2004). Efficiency of repair of an abasic site within DNA clustered damage sites by mammalian cell nuclear extracts. *Biochemistry* **43**: 11017–11026.

McManus KJ, Hendzel MJ. (2005). ATM-dependent DNA damage-independent mitotic phosphorylation of H2AX in normally growing mammalian cells. *Mol Biol Cell* **16**: 5013–5025.

Mischo HE, Hemmerich P, Grosse F, Zhang S. (2005). Actinomycin D induces histone gamma-H2AX foci and complex formation of gamma-H2AX with Ku70 and nuclear DNA helicase II. *J Biol Chem* **280**: 9586–9594.

Mitra S, Kaina B. (1993). Regulation of repair of alkylation damage in mammalian genomes. *Prog Nucleic Acid Res Mol Biol* **44**: 109–142.

Ochs K, Sobol RW, Wilson SH, Kaina B. (1999). Cells deficient in DNA polymerase beta are hypersensitive to alkylating agent-induced apoptosis and chromosomal breakage. *Cancer Res* **59**: 1544–1551.

Redon C, Pilch DR, Rogakou EP, Orr AH, Lowndes NF, Bonner WM. (2003). Yeast histone 2A serine 129 is essential for the efficient repair of checkpoint-blind DNA damage. *EMBO Rep* **4**: 678–684.

Rogakou EP, Boon C, Redon C, Bonner WM. (1999). Megabase chromatin domains involved in DNA double-strand breaks *in vivo*. *J Cell Biol* **146**: 905–916.

Rogakou EP, Nieves-Neira W, Boon C, Pommier Y, Bonner WM. (2000). Initiation of DNA fragmentation during apoptosis induces phosphorylation of H2AX histone at serine 139. *J Biol Chem* **275**: 9390–9395.

Rogakou EP, Pilch DR, Orr AH, Ivanova VS, Bonner WM. (1998). DNA double-stranded breaks induce histone H2AX phosphorylation on serine 139. *J Biol Chem* **273**: 5858–5868.

Soldani C, Scovassi AI. (2002). Poly(ADP-ribose) polymerase-1 cleavage during apoptosis: an update. *Apoptosis* **7**: 321–328.

Stiff T, O'Driscoll M, Rief N, Iwabuchi K, Lobrich M, Jeggo PA. (2004). ATM and DNA-PK function redundantly to phosphorylate H2AX after exposure to ionizing radiation. *Cancer Res* **64**: 2390–2396.

Takai H, Smogorzewska A, de Lange T. (2003). DNA damage foci at dysfunctional telomeres. *Curr Biol* **13**: 1549–1556.

Tibbles LA, Woodgett JR. (1999). The stress-activated protein kinase pathways. *Cell Mol Life Sci* **55**: 1230–1254.

Wang H, Wang M, Bocker W, Iliakis G. (2005). Complex H2AX phosphorylation patterns by multiple kinases including ATM and DNA-PK in human cells exposed to ionizing radiation and treated with kinase inhibitors. *J Cell Physiol* **202**: 492–502.

Ward IM, Chen J. (2001). Histone H2AX is phosphorylated in an ATR-dependent manner in response to replicational stress. *J Biol Chem* **276**: 47759–47762.

Xu B, Kim ST, Lim DS, Kastan MB. (2002). Two molecularly distinct G(2)/M checkpoints are induced by ionizing irradiation. *Mol Cell Biol* **22**: 1049–1059.

Yan Y, Black CP, Cowan KH. (2007). Irradiation-induced G_2/M checkpoint response requires ERK1/2 activation. *Oncogene* **26**: 4689–4698.

Supplementary Information accompanies the paper on the Oncogene website (http://www.nature.com/onc)